NASA Technical Memorandum 83027

Analytical Calculation of a Single Jet in Crossflow and Comparison With Experiment

(NASA-TM-83027) ANALYTICAL CALCULATION OF A SINGLE JET IN CROSSFLOW AND COMPARISON WITH EXPERIMENT (NASA) 15 p HC A02/MF A02
CSCL 21E
N83-14127
Unclas
G3/07 02213

Russell W. Claus
Lewis Research Center
Cleveland, Ohio

Prepared for the
Twenty-First Aerospace Sciences Conference
sponsored by the American Institute of
Aeronautics and Astronautics
Reno, Nevada, January 10–13, 1983

NASA

ANALYTICAL CALCULATION OF A SINGLE JET IN CROSSFLOW AND COMPARISON WITH EXPERIMENT

ORIGINAL PAGE IS
OF POOR QUALITY

Russell W. Claus

National Aeronautics and Space Administration
Lewis Research Center
Cleveland, Ohio 44135

E-1462

Abstract

A series of calculations of a jet in crossflow using a three-dimensional finite difference model of the Navier-Stokes equations were made on a series of progressively finer grids. With a reasonable number of grid points (40x30x20), calculated jet penetration and mixing characteristics were found to compare favorably with the experimental measurements of Crabb, Durao, and Whitelaw. The calculated results were grid dependant (i.e., numerical or false diffusion was present in the result). A finer grid calculation indicated that turbulence model deficiencies may become more noticeable in the calculated results as the magnitude of numerical diffusion is reduced.

Introduction

With the increasing costs of combustor development testing, a great deal of interest has focused on the use of numerical models to screen design changes or develop new combustor concepts. This type of computer-based design process now appears to be feasible through the use of three-dimensional combustor performance models.[1,2] Ultimately, these models may be used to greatly improve the durability and reliability of gas turbine combustors.

A number of major restrictions must be overcome before this type of design methodology can be adopted. First, the proper physics must be incorporated into the differential equations used in the combustor model. Second, numerical methods must accurately solve these differential equations. Finally, the accuracy of the resulting code must be assessed against fundamental data, and improvements must be made to the code to alleviate identified deficiencies.

Currently available three-dimensional combustor performance models have yet to be thoroughly assessed. A few comparisons have been made with actual combustor hardware,[3] but these have not been conclusive. A more logical first step is to examine the extent to which three-dimensional hydrodynamic processes can be calculated. One flow field of this type for which a great deal of experimental data exist is jets in crossflow.

Jets in crossflow are particularly relevant to the gas turbine combustor designer. Cooling air jets (dilution jets) are used to control the hot-gas temperature profile entering the turbine. They are also used to set up aerodynamic patterns within the combustor, (which promote mixing and control local burning zone stoichiometry). As a result, the jet penetration and mixing characteristics of jets in crossflow are of primary concern in the combustor design process.

There have been a number of previous calculations of jets in crossflow,[4,5,6]; however, these studies have been limited by two main factors. First, although a great deal of experimental data exist, rarely have important parameters such as the turbulence field, inlet velocity profiles, and jet mixing characteristics been fully measured. This limits the flow field quantities one can compare and imposes the need to assume inlet boundary conditions for the calculation. Recent measurements greatly reduce this problem.[7] Second, core storage and economy requirements have limited previous calculations to coarse grid systems. This results in some numerical error being present in the computed solution, which can possibly call into question any conclusions drawn from these studies.

The present report expands on this previous work by employing a series of progressively finer grid systems to calculate the single jet in crossflow experimentally measured by Crabb, Durao and Whitelaw.[7] These experimental measurements provide a fairly complete collection of velocities, turbulence intensities, and jet concentration profiles with measurements of the inlet field. The use of a series of progessively finer grid systems allows a differentiation between numerical errors and the hydrodynamic modeling assumptions embodied in the three-dimensional combustor code.[1] The results of this comparison will provide additional insight into the deficiencies of the turbulence model and the code numerics.

Mathematical Formulation

Symbols

U_i	Mean velocity
u_i	Fluctuating velocity about mean
U_∞	Mainstream velocity
Re_c	Cell Reynolds number = $U \Delta x/\nu$
K	Turbulence kinetic energy = $1/2(u^2 + v^2 + w^2)$
ϵ	Turbulence energy dissipation rate
$\bar{\theta}/\bar{\theta}_j$	Normalized mean jet fluid concentration level =1 at jet orifice; = 0 in main stream before jet

Finite Difference Model

The finite difference model employed in this study is similar in construction to those previously reported.[1,2] It provides the capability to analyze steady-state, three-dimensional, elliptic, turbulent, incompressible flow fields. Only the pertinent features of the code will be reviewed here as the literature[1,5] is available for further details.

The governing equations include

Continuity

$$\frac{\partial U_i}{\partial x} = 0 \qquad (1)$$

ORIGINAL PAGE IS
OF POOR QUALITY

Momentum

$$\underbrace{U_i \frac{\partial U_j}{\partial x_i}}_{\text{Convection}} = \underbrace{-\frac{1}{\rho}\frac{\partial p}{\partial x_j}}_{\text{Pressure gradient}} + \underbrace{\frac{\partial}{\partial x_i}\left(\frac{\mu}{\rho}\frac{\partial U_j}{\partial x_i} - \overline{u_i u_j}\right)}_{\text{Diffusion}} \quad (2)$$

Scalar Transport

$$\underbrace{U_i \frac{\partial \phi}{\partial x_i}}_{\text{Convection}} = \underbrace{\frac{1}{\rho}\left(\frac{\partial}{\partial x_i}\frac{\mu}{\sigma_t}\frac{\partial \phi}{\partial x_i} - \overline{u_i \phi}\right)}_{\text{Diffusion}} \quad (3)$$

Turbulence Model

$$\overline{u_i u_j} = \frac{2}{3}\frac{\delta_{ij}}{\rho}K - \frac{\mu_t}{\rho}\left(\frac{\partial U_i}{\partial x_j} + \frac{\partial U_j}{\partial x_i}\right) \quad (4)$$

$$\mu_t = C_\mu \rho \frac{k^2}{\epsilon} \quad (5)$$

$$\overline{u_i \phi} = -\frac{1}{\rho}\frac{\mu_t}{\sigma_t}\frac{\partial \phi}{\partial x_i} \quad (6)$$

where K and ϵ are the kinetic energy and dissipation rate of turbulence energy defined by

$$U_i \frac{\partial K}{\partial x_i} = \frac{1}{\rho}\frac{\partial}{\partial x_i}\left(\frac{\mu_t}{\sigma_k}\frac{\partial K}{\partial x_i}\right) - \overline{u_i u_j}\frac{\partial U_j}{\partial x_i} - \epsilon \quad (7)$$

$$U_i \frac{\partial \epsilon}{\partial x_i} = \frac{1}{\rho}\frac{\partial}{\partial x_i}\left(\frac{\mu_t}{\sigma_\epsilon}\frac{\partial \epsilon}{\partial x_i}\right) - C_{\epsilon 1}\frac{\epsilon}{K}\overline{u_i u_j} - C_{\epsilon 2}\frac{\epsilon^2}{K} \quad (8)$$

where capitals indicate mean quantities and small letters indicate fluctuating quantities. The above equations correspond to the turbulence model of Jones and Launder.[8] The constants used in the turbulence model include

$$C_\mu = 0.09,\ C_{\epsilon 1} = 1.44,\ C_{\epsilon 2} = 1.92,$$

$$\sigma_K = 1.0,\ \sigma_\epsilon = 1.3,\ \text{and}\ \sigma_t = 0.9$$

Solution Procedure

The governing equations are represented by finite difference approximations on a staggered grid system.[9] Hybrid differencing of the convective terms was used to obtain stable, wiggle-free solutions. Central differencing was used for the other terms in the modelled equations. Each iteration of the solution begins with the finite difference forms of the momentum equation being sequentially solved. A Poisson pressure equation is then used to compute the pressure field. This in turn is used to "correct" the velocity field to maintain continuity. Following this, the equations for K, ϵ and ϕ (in this case equals normalized jet fluid concentration) are solved using the corrected velocity field. Iteration on the computed flow field is continued until the sum of the mass residuals is a low value, typically less than 1 percent. This comprises the SIMPLE (Semi Implicit Pressure Linked Equations) algorithm as developed by Spaulding.[10]

Boundary Conditions. Inflow conditions are of the Dirchlet type with the main flow introduced approximately two and one-half jet diameters upstream of the jet injection point. Jet boundary conditions were interpolated from the measurements[7] unless otherwise stated. The rms turbulence intensity was chosen from experimental measurements as a uniform 7 percent of the jet velocity and the inlet length scale was based on 0.03 of the jet diameter. The downstream boundary condition was located approximately 14 jet diameters downstream of the jet injection point.

Cross stream boundary conditions in the z direction (see Fig. 1) were modified from the original code to allow symmetry at the end points. The original code provided for cyclic boundary conditions at the end points, which would have required the use of twice as many grid points to analyze a jet in crossflow. The provision of symmetry permitted the calculation to be bounded by the jet centerline.

Grid Refinement. Hybrid differencing of the convective terms (see eq. (2) in the governing equations requires that some form of grid refinement be used to obtain reasonably accurate solutions. Hybrid differencing is a scheme whereby the type of difference formula employed is dependent on the Reynolds number of the computational cell (Re_c). Second-order accurate central differencing is used when $|Re_c| < 2$. First-order accurate upwind differencing is used when $|Re_c| > 2$. For calculations of practical concern to combuster designers, it is impractical to add enough grid points to maintain a Re_c limit of 2. As a consequence, the computational domain is predominantly upwind differenced resulting in a significant truncation error. The order of this truncation error is similar to the diffusive terms in the governing equations, hence, the name "numerical" or "false diffusion." To minimize the contribution of this numerical error term to the computed solution, the grid was refined employing the method previously demonstrated and briefly summarized here.[11]

Taking a Taylor series expansion of each convective term in the axial momentum equation, the truncation series can be evaluated. For example, the convective term $\partial U^2/\partial x$ has a truncation error of

$$T = \left[\frac{1}{2!}\frac{d^2U^2}{dx^2}\delta x + \frac{1}{\beta!}\frac{d^\beta U^2}{dx^\beta}\delta x^{\beta-1}\right]_{\beta=2n}$$

where n is an integer. If the initial term in this series is used as a measure of the numerical diffusion, the grid can be adjusted to minimize the influence of this false diffusion term in the solution of the overall equation. This is done by making a preliminary calculation of the flow field, and from this computed field the initial term in the truncation series is approximated using central differencing. The net truncation error is then obtained by adding together the initial truncation error for all convective terms. The absolute value of this net convection truncation error is then compared with the magnitude of the other terms (pressure gradient and net convection) in the equation, which are also evaluated using central differences. This comparison should then be made at each grid point in the three-dimensional domain. In theory, additional grid points are then added until the net contribution of the truncation terms is small compared with

ORIGINAL PAGE IS
OF POOR QUALITY

the other terms in the equation. This would then result in a grid-independant solution, given that the higher order truncation terms tend toward zero and that this procedure is applied to each equation solved. More precisely, the solution will be second-order accurate.

This alone does not guarantee an accurate finite difference solution of the governing equations. Castro[12] has shown that when both upwind and central differencing are applied to the solution of the one-dimensional convection-diffusion equation, at high cell Reynolds numbers ($|Re_c| > 2$) upwind differencing is more accurate. In fact, it is this rationale which has led to the use of hybrid differencing.[13] This can be highly misleading, however, when extended to two or three-dimensional flows.[14] The only instance where hybrid differencing may be valid is when the grid structure can be alined directly along flow streamlines. Ad hoc attempts to aline the rectangular grid system to flow streamlines are not likely to result in improved computational accuracy.

Aside from the question of whether or not second-order accuracy is better than first-order accuracy, it is apparent that if the real effects of the turbulence closure are to be observed in the computed solution, the contribution of numerical diffusion must be minimized. Otherwise the physical diffusion of the turbulence model may be overwhelmed by numerical diffusion contributed by the truncation error. For this reason, the grid refinement procedure was employed. Unfortunately, enough grid points could not be added to the three-dimensional flow field to demonstrate a second-order accurate solution; however, (as will be noted in the section Results) numerical diffusion could be reduced enough so that the physical deficiencies of the turbulence model could be partially discerned.

The use of a rational grid refinement scheme is especially important in three-dimensional flows where the luxury of doubling the number of grid points in all directions cannot be afforded both from the standpoint of excessive computing times and core storage requirements. The grid refinement procedure has the advantage of demonstrating in which areas of the flow field the grid can most effectively be refined to minimize false diffusion.

Flow Configuration. A schematic drawing of the free jet coordinate system is given in Fig. 1. The x (axial) direction is oriented in line with the mainstream flow. The free jet is injected along the y direction and normal to the main-stream flow. The cross stream direction is along the z axis.

Calculations were made for the flow conditions corresponding to the experimental measurements of Crabb, Durao, and Whitelaw.[7] The main-stream flow was specified at a uniform 12 m/s. The dilution jet to main-stream velocity ratio was 2.3. Boundary conditions in the z and y direction were located far enough away from the jet orifice to avoid having any effect on the computed flow field.

Results and Discussion

In the following discussion, experimental versus calculated results are shown for three different grid systems: A coarse grid (20x20x12 grid points), a medium grid (40x30x20), and a fine grid (90x40 x22). To determine where the grid should be refined, the grid refinement procedure mentioned earlier was used. The purpose of this examination of various finite difference grid systems is two-fold. First, the use of several grid systems insures that conclusions drawn from the calculated results are not anomalies of the number of grid points used. Second, it is important to quantify the trade-off involved between numerical accuracy and computational expense. Absolute precison may not be warranted in engineering calculations, where the inlet parameters to the calculation may be uncertain and only some gross features of the flow field may be of interest. But the converse danger of using too coarse a grid system must be avoided, otherwise important flow field characteristics may be masked. By using several grid systems, the trade-off between accuracy and computational expense is illustrated.

The main factor to be observed in the three different grid calculations is the extent to which numerical or false diffusion affects the calculated results. Other factors such as inlet boundary conditions and convergence criteria were maintained constant for each calculation.

Coarse Grid. Comparison between a coarse grid calculation of the free jet flow field and the experimental measurements[7] is shown in Fig. 2. The grid system, 20x20x12 (number of points in the X x Y x Z directions), is completely inadequate to accommodate the steep velocity gradients in the flow field. The axial velocity peak evident in the experimental measurements at Y/D = 2.5 is essentially missing in the computed flow field (see Fig. 2(a)). The same effect is evident further downstream in Fig. 2(b), but the general S-shaped nature of the flow is fairly well-predicted. The profiles of normalized jet fluid coincide fairly well but the calculated peak indicates that the jet is slightly over-penetrating (see Fig. 2(c)).

A qualitative examination of the cross-stream vortex formed in the course grid calculation is displayed by velocity vector plots (see Fig. 3). The vortex structure is just being formed at a cross section bisecting the jet orifice (see Fig. 3(a)). Just downstream of the jet orifice, the vortex can be seen to have gained strength (see Fig. 3(b)). The center of the vortex has also moved slightly closer to the jet centerline (at Z/D = 0) The vortex can be seen to have expanded in size while the center is slightly displaced outward (see Fig. 3(c)). In a qualitative sense, this vortex structure agrees with the measurements of Ref. 7. The loci of the vortex center could be traced from the experimental measurements to be drawn back into the wake region behind the jet, and then be transported outward further downstream. However, the precise location of this vortex center and its movement is not well-predicted. For example, the experimental measurements indicate that the outward movement should occur around X/D = 3.25. The calculations clearly predict this will occur much closer to the jet orifice.

A consequence of this strong, calculated vortex structure can be seen in Fig. 4. Here the experimental and calculated normalized jet concentration profiles at an axial location of X/D = 8 are compared. The strong cross stream vortex causes the maximum of the jet concentration to occur off the jet centerline. This physically agrees with the experimental results; however, the strong cross

ORIGINAL PAGE IS
OF POOR QUALITY

stream vortex may also augment the penetration of jet fluid in the Y direction with the net result leading to a poor comparison between calculated and experimental results.

Medium Grid. Additional grid points were added to the computational domain to observe whether any improvement over the coarse grid calculation could be obtained. A comparison between the calculated and experimental results can be seen in Fig. 5. The use of 40x30x20 grid points provided a greatly improved accommodation of the velocity gradients in the flow field. Axial velocity profiles at two different axial locations display an improved comparison between calculated and experimental results (Figs. 5(a) and (b)). In general, the jet penetration appears to coincide well with the experimental measurements. In Fig. 5(c) the axial turbulence intensity ($\sqrt{u^2}$) is compared at an axial location of X/D = 2. The magnitude of the axial turbulence intensity compares favorably with the experiment around Y/D = 1.5, but is underpredicted elsewhere.

The moderately good agreement shown in Fig 5(c) can be misleading. Explicit data are not available at this axial location, but the measurements of Ref. 7 indicate that in the jet wake region, the magnitude of the cross stream (Z direction) turbulent fluctuations is much greater than the magnitude of the axial fluctuations (X direction). The isotropic turbulence model used in the calculation procedure assumes an equal magnitude of turbulence intensity in all directions; therefore, the cross-stream fluctuations are likely to be significantly underpredicted by this model. This is a common problem with the isotropic assumption and has been noted elsewhere.[5]

In Fig. 5(d) profiles of axial turbulence intensity and normalized jet fluid concentration are shown at an X/D of 6. Here, the turbulence intensity is consistently underpredicted and the same isotropic turbulence limitation is likely to be true. However, the isotropic assumption should be less restrictive since the flow will have a tendency toward isotropy far downstream of the jet orifice.

One of the interesting experimental findings of Ref. 7 is that the profiles of mean axial velocity and jet fluid concentration do not coincide. The free-stream fluid is accelerated around the jet and causes the velocity peak around Y/D = 3.5 (see Fig. 5(b)). The concentration of jet fluid peaks around Y/D = 2.8 (i.e., in the wake region). Experimentally, the jet fluid concentration profiles were found to coincide more appropriately with the axial turbulence intensity profile, instead of the axial velocity profile. Both trends are well-reproduced in the calculated results (Figs. 5(b) and (c)).

Further verification of the accurate prediction of jet penetration can be seen in Fig. 6. Calculated velocity vectors are displayed against an empirical correlation for jet penetration.[15] The velocity vectors match the empirical trajectory quite well. Another positive feature of the computed flow field can be seen in this figure. The upwelling, or positive V velocity, that can be seen in the recirculation zone behind the jet qualitatively agrees with the results of Ref. 7.

A less favorable aspect of the computed flow field can be seen in the velocity vector plot of Fig. 7. Here the y-z plane at an axial location of x/D = 2 displays an unusual vortex structure. Two coflowing vortices are embedded in the overall cross-stream vortex. This structure, which was not apparent in the coarse grid results (Fig. 3), cannot be supported by the experimental measurements. It appears to be a nonphysical artifact of the calculation, which may be related to the isotropic turbulence model. If the calculated cross stream turbulence intensity were greater, these two vortices might collapse into one large cross-stream vortex.

Despite this nonphysical aspect of the velocity field, an excellent agreement exists between calculated and experimental results for the normalized jet fluid concentration profiles at X/D = 8 (see Fig. 8). The most surprising feature of this agreement is the accuracy of the cross stream (z direction) transport of jet fluid. As noted earlier, the cross stream fluctuations could be inferred to be larger in magnitude than the axial turbulent fluctuations in the jet wake region. Therefore, the inadequacy of the isotropic turbulence model should have exhibited itself as a lack of turbulent diffusion in the z direction. The reason for this discrepancy is a result of numerical or false diffusion, as will be made clear in the next series of calculations.

Fine Grid. The results of a fine grid calculation (90x40x22) are compared against experimental measurements in (Fig. 9). Here the addition of grid points has slightly improved the axial velocity comparisons (Fig. 9(a)) while lessening the agreement on jet concentration profiles (Fig. 9(b)). The recirculation zone velocity is matched more closely than the previous results and the velocity peak at Y/D = 2.4 is slightly closer to the experimental value (see Fig. 9(a)). The calculated jet concentration profiles indicate a lack of jet spreading in the Y direction. This is especially noticeable in the region around Y/D = 3 - 4. The 0.20 contour does not spread in the Z direction as far as previous results. The maximum penetration is about Z/D = 1.0 as opposed to an experimental value of about 1.3 (1.3 is also the maximum penetration determined in the medium grid calculation). The 0.10 contour does spread correctly in the Z direction.

The results (Fig. 9) are still grid dependent and the reason for this is seen in Fig. 10. Three of the terms in the axial momentum equation (eq. (2)) are shown at an axial location of X/D = 1.3 near the jet centerline. (The diffusion term is excluded for clarity). These terms were evaluated using central differencing of the computed flow field in a manner consistent with the procedure defined in the section Grid Refinement. The main feature of the indicated profiles is that the convection truncation error (numerical or false diffusion term) is negligible for much of the flow field but becomes quite significant around a Y/D of 2. The axial velocity profile (Fig. 10(b)) corresponds to the same location as that in Fig. 10(a). The truncation errors can be seen to correspond to the velocity peak of the fluid accelerating around the jet. This is a region of very steep velocity gradients, which causes the locally large truncation errors. The development of the

ORIGINAL PAGE IS
OF POOR QUALITY

velocity peak is largely controlled by numerical diffusion (Figs. 10(a) and (b)).

Truncation errors are even more serious in the solution of the scalar transport equation (eq. 3). (This equation is solved to determine jet fluid concentration profiles - Fig. 9(b). In the solution of this equation, the convection terms (determined by hybrid differencing) are set equal to the diffusion terms (determined by central differencing). There is no pressure gradient term. This results in the convection truncation error having a large impact on the solution of the equation. For example, Fig. 11 displays the magnitude of the convection and truncation terms in the scalar transport equation at X/D = 1.9 and Z/D = 0.9. The truncation terms contribute significantly to the computed result. This explains how the jet fluid concentration profiles can spread in a manner not consistent with the physics of the turbulence model. The solution is so badly swamped by numerical diffusion in some regions of the flow field that it almost controls the computed results. It is only in the fine grid results (Fig. 9(b)) that an indication is given of what an error-free solution might yield. The concentration profiles would not spread quite so far in the Y or Z direction as was shown in the 0.20 concentration profile. The agreement seen in the 0.10 profile is simply a result of the lack of grid points in this region of the flow field.

Computing Times. The coarse grid calculations displayed in this report required approximately 20 CPU min of computing time on an IBM model 370-3033. The medium grid calculations required about 2 CPU hours and the fine grid calculations about 10 CPU hr.

Summary. Comparisons between experimental and calculated results for three different grid systems have been presented. All grid systems were subject to some numerical error (numerical diffusion). The coarse-grid calculations exhibited a high degree of numerical diffusion resulting in a obscuration of the jet velocity peak, especially near the jet orifice. The medium-grid calculations exhibited noticeably less numerical diffusion with an underprediction of the magnitude of the jet peak velocity but a correct penetration trajectory. The jet concentration profiles for this grid compared very well with experiment. The fine-grid calculation exhibited a slightly better comparison of the jet peak velocities but a worse correspondence between experimental and calculated jet concentration profiles.

All calculations provided a qualitative prediction of some features of the single jet flow field. For the cross-stream vortex, the agreement became less qualitative as additional grid points were added, which is in physical agreement with the turbulence model.

Previous calculations of jets in cross flow[4] have indicated an excellent correspondence with experimentally determined jet trajectories. It is postulated that the pressure field essentially controls jet penetration and, hence, any inaccuracies in the turbulence closure or the differencing scheme are of lesser importance.[7] From the results of this report, it appears that this may or may not be true, depending on the number of grid points used in the calculation. Coarse grid calculations indicated some overpenetration of the jet, but with a reasonable number of grid points the jet trajectory was well predicted.

Equally important are the jet fluid mixing characteristics; and these were found to be very sensitive to numerical and turbulence model inaccuracies. Unfortunately, the response of these variables to grid refinement is only sluggish at best.

Concluding Remarks

What is illustrated quite clearly is the need for an improved numerical scheme to eliminate numerical diffusion. A variety of techniques[16,17] may provide a resolution to this problem. However, this is not to say that the current three-dimensional combustor models cannot be used to make engineering calculations. For the flow field in this investigation, the medium grid (40x30x20 grid points) provided a good compromise between computational expense and accuracy. For other types of flows this would doubtless vary and currently can only be determined by a post analysis of the truncation error.

Conclusions

Employing a three-dimensional finite-difference model to analyze the jet flow field,[7] the following conclusions were determined:

1. With a reasonable number of grid points (approximately 40x30x20), calculated jet penetration and concentration profiles agreed well with experimental measurements.

2. For the cross-stream vortex, the agreement between experimental and calculated results became less qualitative as additional grid points were added, indicating a defiency of the isotropic turbulence model.

3. The calculated results of the finest grid examined (90x40x22) were grid-dependent. An improved numerical scheme is required to remove the effects of numerical diffusion for the flow geometry examined.

References

1. Mongia, H.C., and Reynolds, R.S., "Combustor Design Criteria Validation, Volume III - User's Manual," USARTL-TR-78 -55C, Feb. 1979.

2. "Design and Development of Gas Turbine Com bustors Basic Computing Section, Volume III User's Manual," NREC Report No. 1420-3, 1981.

3. Serag-Eldin, M.A.S. and Spaulding, D.B., "Computation of Three Dimensional Gas Turbine Combustion Chamber Flows, "ASME Journal of Engineering for Power, Vol. 101, No. 2, July 1979, pp. 327-336.

4. Patankar, S.V., Basu, D.K. and Alpay, S.A., "Prediction of Three Dimensional Velocity Field of a Deflected Turbulent Jet, "ASME Journal of Fluids Engineering, Vol. 99, No. 4, Dec. 1977, pp. 758-762.

5. Jone, W.P., and McGuirk, J.J., "Computation Of a Round Turbulent Jet Discharging into a Confined Cross-Flow," Turbulent Shear Flows II, Springer Verlag, New York 1979, pp. 233-245.

6. Khan, Z.A., McGuirk, J.J. and Whitelaw, J.J., "A Row of Jets Discharging in Cross-Flow," Fluid Dynamics of Jets with Applications to V/STOL, AGARD-CP-308, 1982.

7. Crabb, D., Durao, D.F.G. and Whitelaw, J.J., "Round Jet Normal to a Cross-Flow, "ASME Journal of Fluids Engineering, Vol. 103, No. 1, Mar. 1981, pp. 142-153.

8. Jones, W.P., and Launder, B.E., "The Prediction of Laminarization With a Two-Equation Model of Turbulence," International Journal of Heat and Mass Transfer, Vol 15, No. 2, Feb. 1972, pp. 301-314.

9. Harlow, F.H. and Welch, J.E., "Numerical Calculation of Time-Dependent Viscous Incompressible Flow of Fluid with Free surface, "Physics of Fluids," Vol 8, No.12, Dec. 1965, pp. 2182-2189.

10. Patankar, S.V. and Spaulding, D.B., "A Calculation Procedure for Heat, Mass and Momentum Transfer in Three-Dimensional Parabolic Flows, "International Journal of Heat and Mass Transfer, Vol. 15, No. 10, Oct. 1972, pp. 1787-1806.

11. McGuirk, J.J., Taylor, A.M.K.P., and Whitelaw, J.H., "The Assessment of Numerical Diffusion in Upwind-Difference Calculations of Turbulent Recirculating Flows. "Third Symposium on Turbulent Shear Flows, Davis, Ca, Sept. 1981.

12. Castro, I.P., "Numerical Difficulties in the Calculation of Complex Turbulent Flows," Turbulent Shear Flows I, Springer-Verlag, New York, 1979, pp. 220-236.

13. Lilley, D.B. and Rhode, D.L., "STARPIC -A Computer Code For Swirling Turbulent Axisymetric Recirculating Flows in Practical Isothermal Combustor Geometries, "NASA CR-3442, Feb. 1982.

14. Domingos, J.J.D. and Lopes, J.M.B., "Numerical Stability and False Diffusion in Recirculating Flows. "Third Symposium on Turbulent Shear Flows, Davis, Ca, Sept 1981.

15. Katotani, Y. and Greber, I., "Experiments on Confined Turbulent Jets in a Cross-Flow," NASA CR-2392, Mar. 1974.

16. Leonard, B.P., "A Stable and Accurate Convective Modeling Procedure Based on Quadratic Upstream Interpolation, "Computer Methods in Applied Mechanics and Engineering, Vol. 19, No. 1, June 1979, pp. 59-98.

17. Raithby, G.D., "Skew Upstream Differencing Schemes for Problems Involving Fluid Flow, "Computer Methods in Applied Mechanics and Engineering, Vol. 9, no. 2, Oct. 1976, pp. 153-164.

ORIGINAL PAGE IS
OF POOR QUALITY

ORIGINAL PAGE IS
OF POOR QUALITY

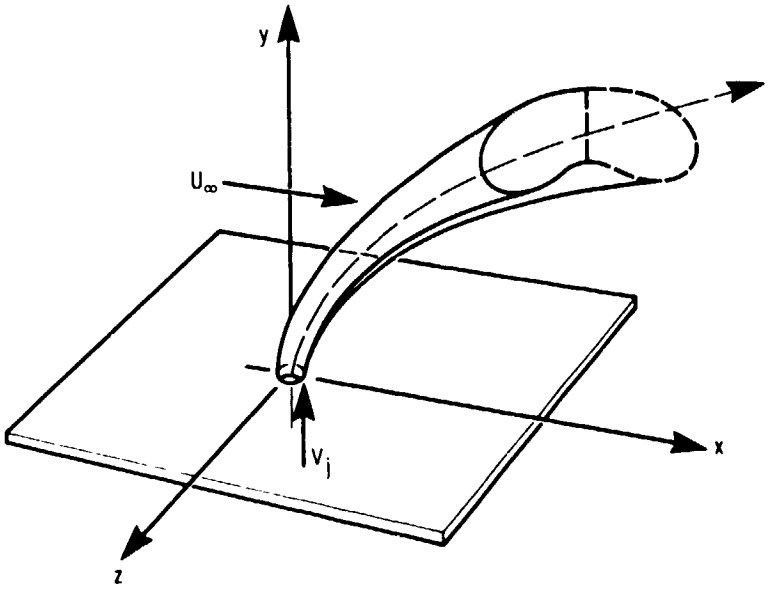

Figure 1. - Schematic drawing of dilution jet coordinate system.

ORIGINAL PAGE IS
OF POOR QUALITY

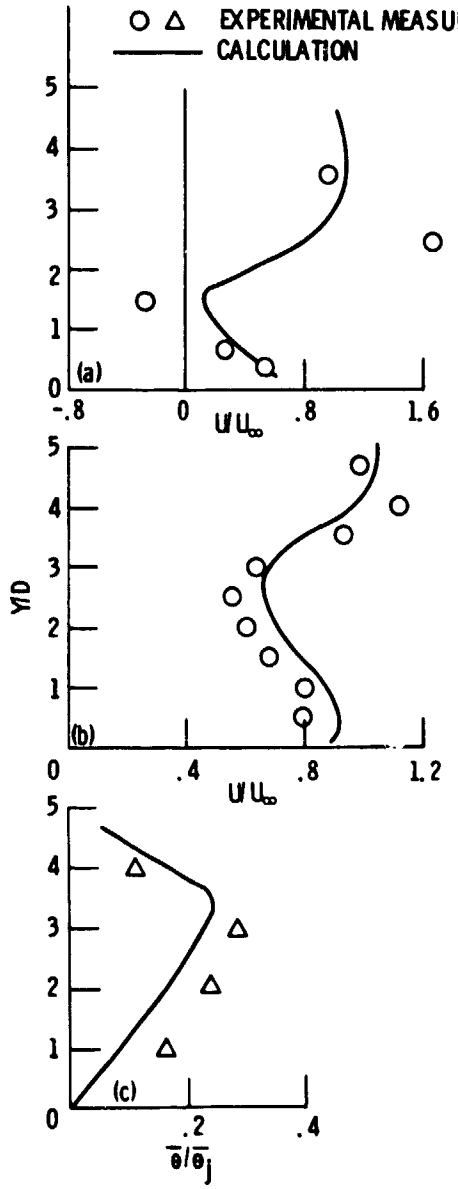

(a) X/D=2.
(b) X/D=6.
(c) X/D=6.

Figure 2. - Coarse grid (20x20x12) calculation of a single, free jet. Velocity profiles at a) X/D=2, b) X/D=6, and c) normalized jet fluid concentration profiles at X/D=6. All profiles shown are through the jet centerline.

ORIGINAL PAGE IS
OF POOR QUALITY

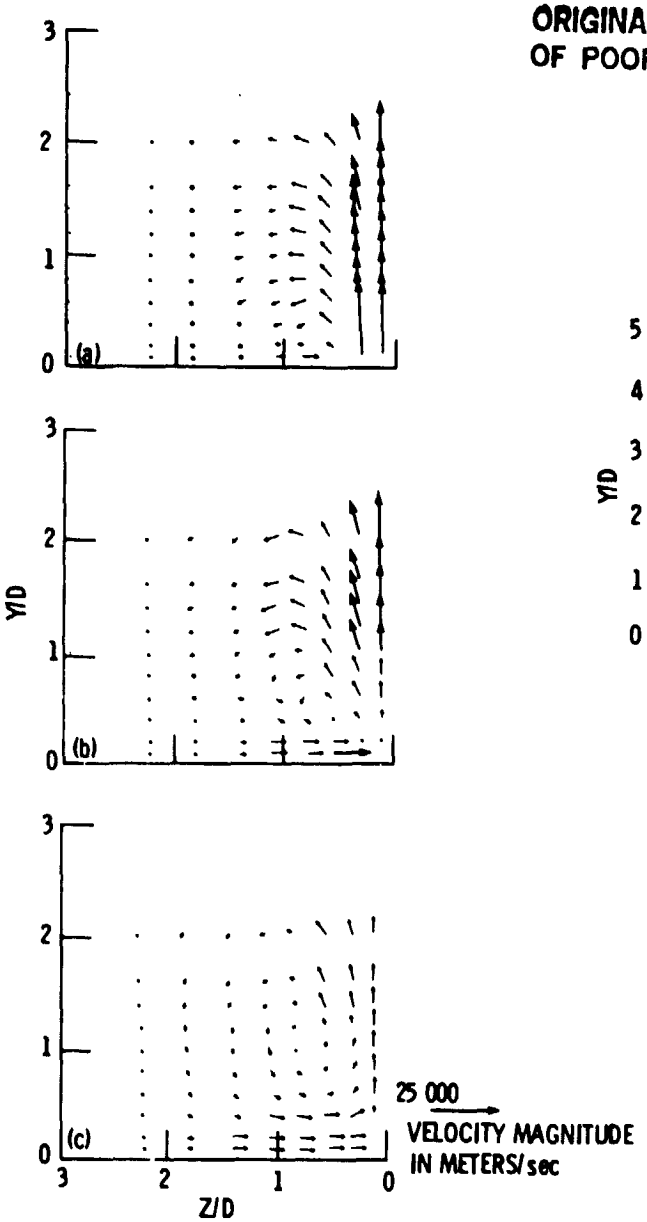

(a) X/D=0. 125.
(b) X/D = 0. 625.
(c) X/D=1. 375.

Figure 3. - Velocity vector plots of a coarse grid (20x20x12) calculation of the single jet flow field displaying the cross-stream vortex.

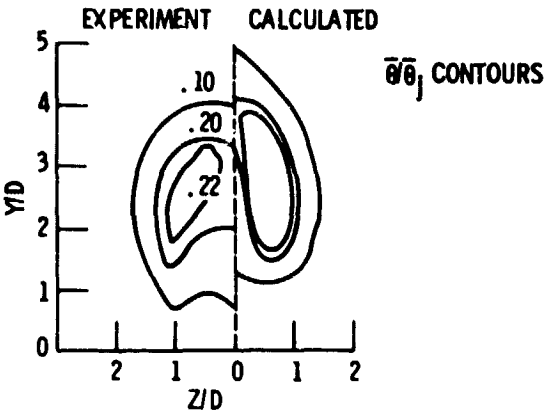

Figure 4. - Coarse grid (20x20x12) calculation of jet fluid concentration profiles and comparison with experiment at X/D=8.

ORIGINAL PAGE IS
OF POOR QUALITY

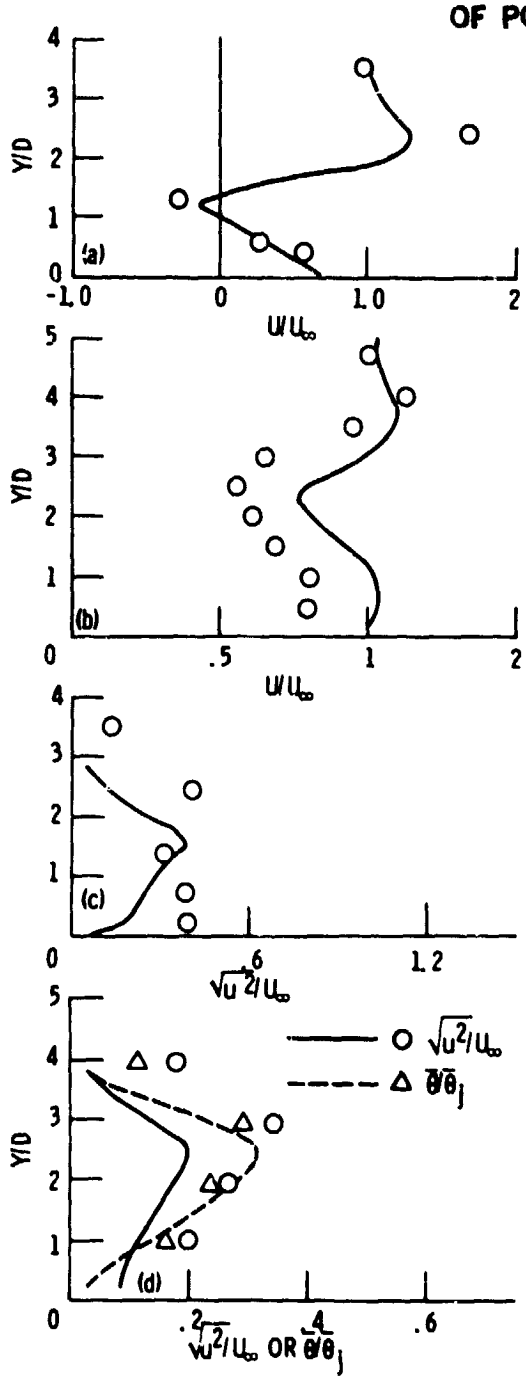

(a) Axial velocity profiles along jet centerline at X/D=2.

(b) Axial velocity profiles along jet centerline at X/D=6.

(c) Turbulence profiles along jet centerline at X/D=2.

(d) Turbulence and jet fluid concentration profiles along jet centerline at X/D=6.

Figure 5. - Medium grid (40x30x20) calculation of single, free jet flow field and comparison with experiment.

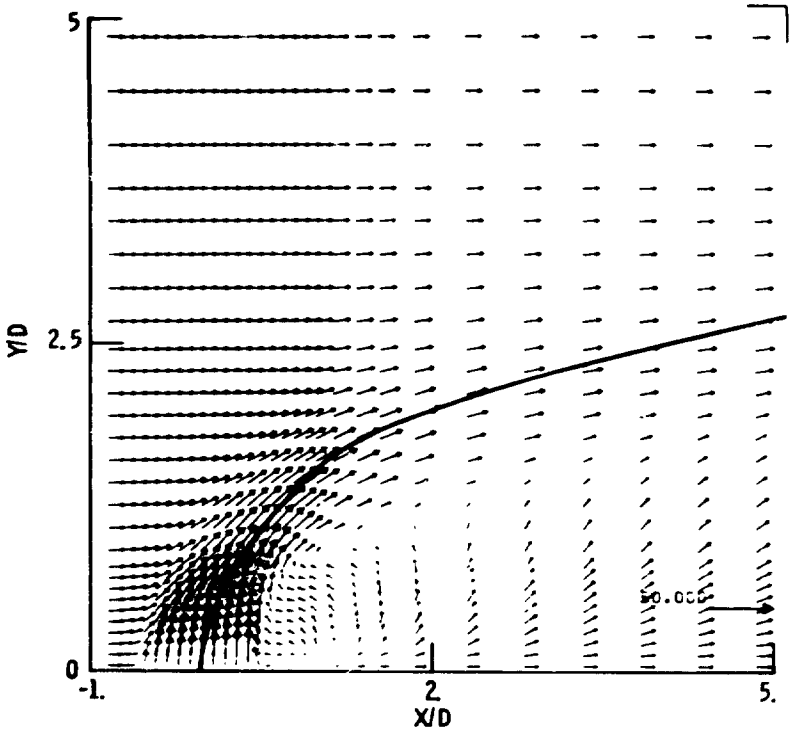

Figure 6. - Medium grid (40x30x20) calculated velocity vectors of single, free jet flow field. Shown is the x-y plane through the jet centerline with the solid line indicating empirical, trajectory correlation of ref. 15.

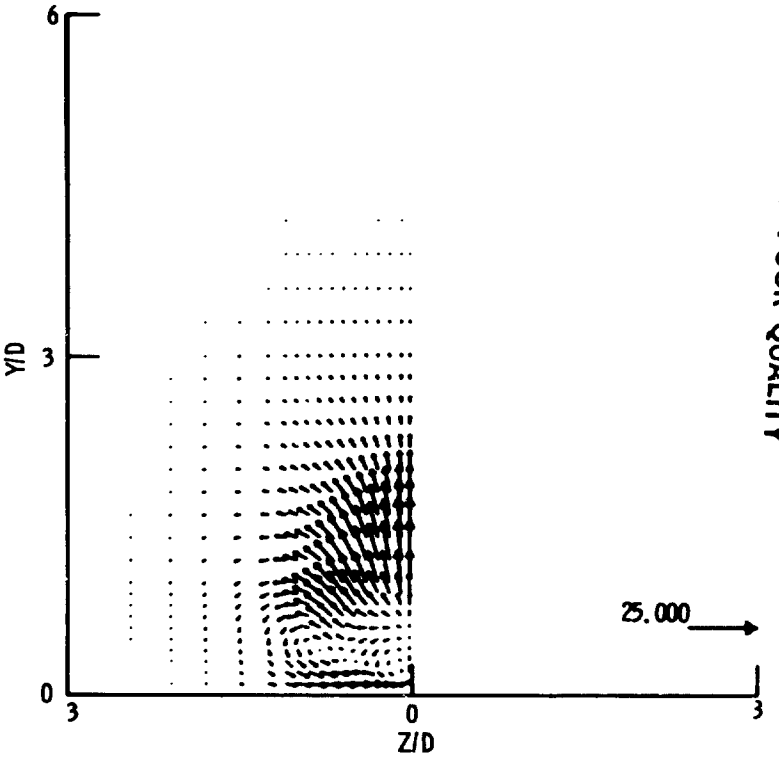

ORIGINAL PAGE IS
OF POOR QUALITY

Figure 7. - Velocity vector plots of a medium grid (40x30x20) calculation of the single jet flow field displaying the cross-stream, double vortex structure at X/D=2

ORIGINAL PAGE IS
OF POOR QUALITY

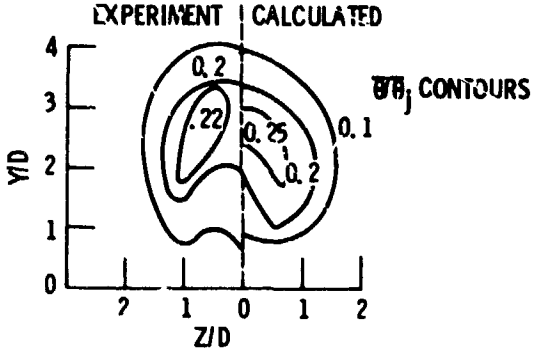

Figure 8. - Medium grid (40x30x20) calculation of jet fluid concentration profiles and comparison with experiment at X/D=8.

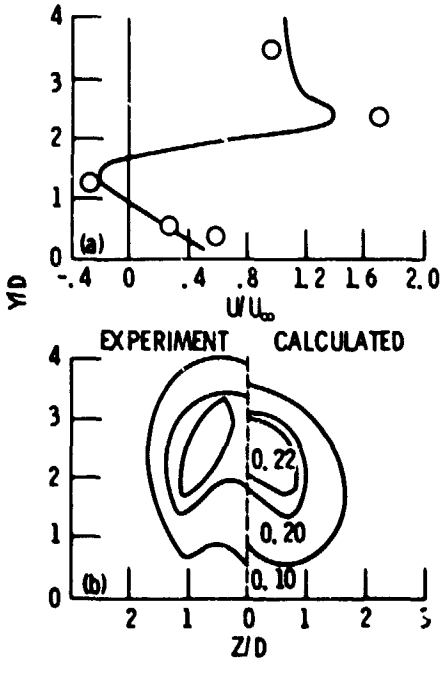

(a) Axial velocity profile at X/D=2.

(b) Jet fluid contration profile at X/D=8.

Figure 9. - Fine grid (90x40x22) calculation of a single jet.

ORIGINAL PAGE IS
OF POOR QUALITY

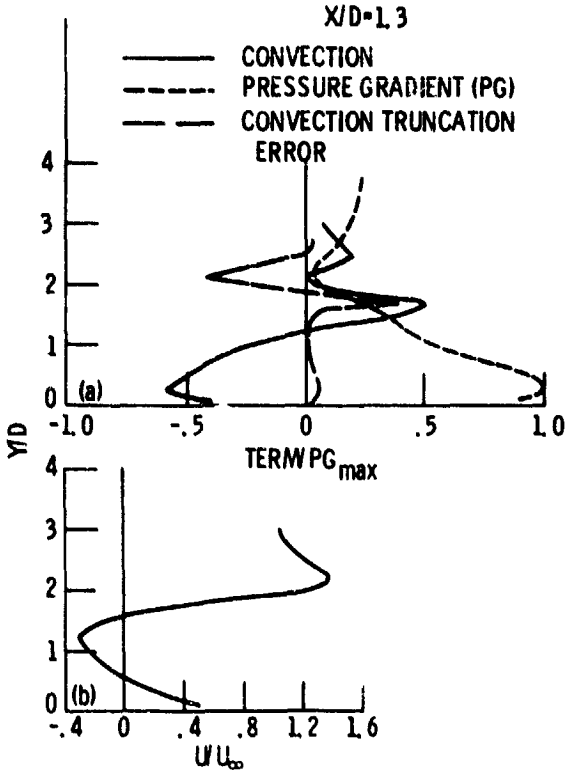

(a) Convection, pressure gradient and convective truncation error at X/D=1.3 near the jet centerline.

(b) Axial velocity at X/D=1.3 near the jet centerline. (Grid 90x40x22.)

Figure 10. - Comparison of the terms in the axial momentum equation.

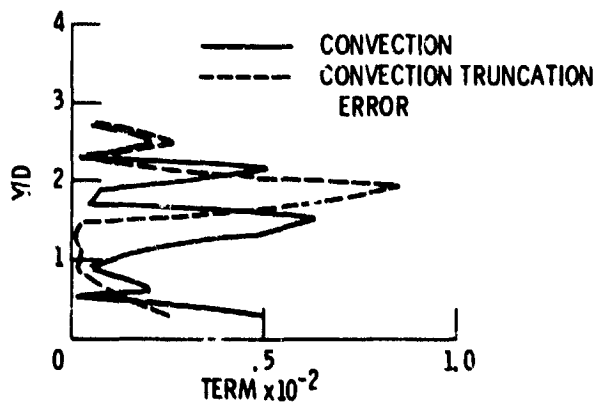

Figure 11. - Comparison of convective terms in the scalar transport equation at X/D=1.9 and Z/D=0.9 (Grid 90x40x22).